Multi-modal MRI analysis for automatic trajectory planning of deep brain stimulation neurosurgery

S. Bériault[1], F. Al Subaie[2], K. Mok[3], A. F. Sadikot[2], and G. B. Pike[1]
[1]McConnell Brain Imaging Centre, Montreal Neurological Institute, Montréal, Québec, Canada, [2]Department of Neurology and Neurosurgery, Montreal Neurological Institute, [3]Neuronavigation Unit, Montreal Neurological Institute

Introduction. A promising treatment for severe Parkinson disease involves the insertion of deep brain stimulation (DBS) electrodes via minimally invasive image-guided neurosurgery. Planning the optimal procedure requires the surgeon to find the best direct path to the subthalamic nuclei (STN) target that avoids critical brain structures (e.g. ventricles, sulci, blood vessels, motor area) to prevent hemorrhages, loss of function and other complications. Currently, this is done by manual inspection of the patient imaging data although there has been recent interest in automating this process[1,2]. In this work, we propose an automatic path planning framework that incorporates several key improvements at every stage of the process: from MRI acquisition to automatic trajectory selection. First, our approach takes advantage of the most recent advances regarding venous and arterial blood vessel imaging with the use of susceptibility weighted imaging (SWI) and time-of-flight (TOF-MRA) protocols. Second, our trajectory analysis software can handle fuzzy datasets (e.g. vesselness filtered data) without the use of a global threshold or of lengthy, iterative, post-processing. Third, our framework meaningfully aggregates several clinical requirements into a single trajectory ranking.

Method. *MRI Acquisition*: Multi-modal MRI datasets were obtained on two healthy subjects using a 3T Siemens TIM Trio using a 32-channel coil. First, a sagittal T1w anatomical scan of the entire head with 1x1x1-mm resolution is obtained using a 3D magnetization-prepared rapid gradient-echo (MP RAGE) sequence (TR=2300ms, TI=900ms, TE=2.98ms, α=9°). Second, a transverse SWI dataset[3] of the brain with 0.5x0.5x1-mm resolution is obtained using a fully flow compensated 3D gradient echo sequence (TR=30ms, TE=20ms, α=12°, BW=120Hz/px, adaptive coil combine). Third, an MRA dataset is obtained with 1x1x1-mm resolution using a 3D multi-slab TOF (4 slabs, 44 slices/slab, transverse acquisition, TR=22ms, TE=3.85ms, α=18°). *Multi-modal data preprocessing:* The STN (target points) are identified via linear registration of the T1w dataset to the ICBM-152 atlas. Entry points to analyze include all head surface voxel found within a user-selectable bounding box starting behind the hairline and ending prior to the motor cortex. Ventricle and sulci segmentation is performed using an in-house atlas-based tissue classification method. SWI and TOF datasets are preprocessed using a 3D multiscale vesselness filtering measure[4]. *Automatic trajectory planning:* For each trajectory, a cost function is calculated separately for each surgical requirement. The cost of a specific voxel is inversely proportional to its distance from trajectory and, for fuzzy datasets, proportional to the actual voxel value. For speed, this search is restricted to voxels found within a 5-mm radius of the trajectory. The maximal cost and sum of costs are extracted and a histogram analysis is performed to rank each trajectory on a [1-100] scale. An aggregated score is then computed for every trajectory using a weighted sum of the numerous individual rankings. A greater weight is given to the maximal cost criterion (over the sum criterion) because almost hitting a critical structure once is more severe than approaching the same critical structure multiple times at a safer distance[1].

Table 1. Comparison of automatic and manual (parentheses) trajectory planning for two subjects

Trajectory	sulci analysis			swi_analysis		Tof analysis		Aggregated Score	Time (min)
	$rank_{max}$	$rank_{sum}$	$dist_{min}$ (mm)	$rank_{max}$	$rank_{sum}$	$rank_{max}$	$rank_{sum}$		
s0_stn_left	2 (25)	1 (44)	3.7 (1.4)	6 (4)	12 (38)	1 (2)	9 (17)	45 (315)	3.5 (30)
s0_stn_right	1 (5)	1 (15)	4.4 (3.0)	14 (7)	13 (27)	2 (1)	28 (30)	69 (121)	4.0 (15)
s1_stn_left	1 (--)	6 (--)	3.0 (0.2)	13 (--)	18 (--)	1 (--)	24 (--)	70 (--)	3.1 (25)
s1_stn_right	1 (12)	2 (17)	3.9 (1.9)	1 (28)	7 (25)	1 (3)	21 (44)	40 (193)	3.3 (20)

Results. Our automatic path planning tool was evaluated by a senior neurosurgery resident and an experienced neurosurgeon. First, the senior resident was asked to perform manual trajectory planning using a commercial neuronavigation system. Paths found manually were then evaluated using our cost function to determine their overall rankings. Table 1 shows that, for all four planning experiments, the computed trajectory almost always exhibits a superior ranking for all individual criteria of sulci and vessel avoidance. The manual trajectory for subject 1's left STN was even rejected by our system because it almost intersects a sulcus. Second, both surgeons were asked to validate the best trajectories identified by our method using 2D and 3D visualization software (e.g. Fig. 1). Each automatic planning experiment lead to a satisfactory trajectory. Our automated method is also fast with ~12000 trajectories analyzed in less than 4 minutes.

Conclusion. Manual path planning, especially with dense multi-modal datasets, is a complex and lengthy process that yields subjective and potentially sub-optimal or even unsafe solutions. This work provides neurosurgeons with an intuitive decision support system for automatic planning of DBS neurosurgeries that aggregates multiple surgical requirements into a single weighted ranking of available trajectories.

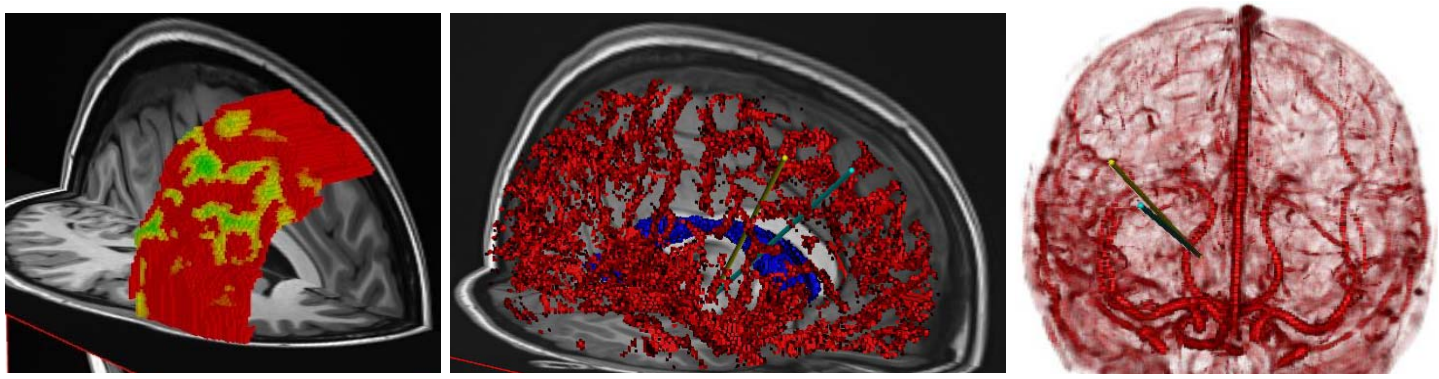

(a) (b) (c)

Fig. 1 3D visualization of critical structures and path planning for subject 0. (a) Color-coded map of entry points to the right STN. (b) 3D view of ventricles (blue) and sulci (red) critical structures, computed trajectory (yellow) and manual trajectory (cyan). (c) 3D view of dense SWI and TOF vesselness filtered data.

References. [1] Brunenberg et al. (2007), MICCAI, 584-92. [2] Shamir et al. (2010), MICCAI, 457-64. [3] Haacke et al. (2009) AJNR Am J Neuroradiol, 30(1), 19-30. [4] Frangi et al. (1998), MICCAI, 130-7.